



Article

On the Structure and Mechanical Properties of Multilayered Composite, Obtained by Explosive Welding of High-Strength Titanium Alloys

Daria V. Lazurenko ^{1,*}, Ivan Bataev ¹, Iulia Maliutina ¹, Ruslan Kuz'min ¹, Vyacheslav Mali ², Maksim Esikov ^{2,3}  and Elena Kornienko ¹

¹ Material Science Department, Novosibirsk State Technical University, K. Marks 20, Novosibirsk 630073, Russia; ivanbataev@ngs.ru (I.B.); julevern@inbox.ru (I.M.); kaf_mm@corp.nstu.ru (R.K.); kornienko_ee@mail.ru (E.K.)

² Laboratory of High Energy Density Physics, Lavrentyev Institute of Hydrodynamics SB RAS, 15 Lavrentyev pr., Novosibirsk 630090, Russia; vmali@mail.ru (V.M.); esmax@ya.ru (M.E.)

³ Department of Gas-dynamic impulse devices, Novosibirsk State Technical University, K. Marks 20, Novosibirsk 630073, Russia

* Correspondence: pavlyukova_87@mail.ru; Tel.: +7-923-245-5243

Received: 29 May 2018; Accepted: 3 July 2018; Published: 6 July 2018



Abstract: One of the ways to simultaneously increase the strength and the fracture and impact toughness of structural materials is by producing multilayered materials. In this paper we discuss the structure and properties of a seven-layer composite obtained by explosive welding of high-strength titanium alloys. The structure of the composite was characterized using light microscopy, scanning electron microscopy (SEM), and transmission electron microscopy (TEM). At the interfaces between plates, formation of waves and vortices was observed. The wave formation is discussed with respect to the kinetic energy loss. The vortices consisted of a mixture of two alloys and possessed a martensitic structure comprising α' and β phases of titanium. Localized plastic deformation occurred along the interfaces during explosive welding by formation of shear bands. The most intensive shear banding occurred in the vicinity of the upper interfaces. The local hardness at the interfaces increased due to the formation of the quenched structures. The interfaces between titanium alloys positively influenced the impact toughness of the composite, which increased in comparison with that of bulk titanium alloys by a factor of 3.5. The strength characteristics of the composite remained at the same level as that of the bulk material (1100–1200 MPa).

Keywords: explosive welding; $\alpha + \beta$ titanium; shear bands; vortices; impact toughness

1. Introduction

Titanium and titanium alloys are widely used structural materials in the aircraft industry, shipbuilding, chemical engineering, medicine, and other industrial sectors which demand a combination of high mechanical properties and unique physical and chemical properties [1]. One of the biggest advantages of titanium alloys is their low specific weight, which in combination with enhanced strength and fatigue characteristics, and high temperature and corrosion resistance, provide the reliable service of titanium products under different loading conditions [2].

One of the most important characteristics defining the quality of titanium alloys is the strength level. Several main methods are currently utilized for strengthening titanium and its alloys. Among them are alloying, heat treatment, and severe plastic deformation [3–6]. The aforementioned methods efficiently increase the ultimate tensile strength (UTS) and the yield strength (YS) of titanium. For example, the UTS of commercially pure (CP) titanium as a rule does not exceed 450 MPa, while the strength of titanium

alloys can reach 1200 MPa. Heat treatment of some high-strength titanium alloys increases the UTS up to 1500 MPa [7]. Equal channel angular pressing (ECAP) increases the UTS of CP titanium by a factor of 2.5 [3–6]. However, an important disadvantage of all these technologies is the decrease of ductility and impact toughness of the material, which negatively affects the reliability of titanium products.

Several approaches can be proposed to resolve a contradiction between strength and toughness of alloys. One of them is the fabrication of laminated composites [8], which significantly improves elongation at fracture, impact toughness, fracture toughness, and fatigue life of materials, maintaining the strength at the initial level [9]. The enhanced crack growth resistance and impact toughness of multilayered metallic materials are provided by the positive influence of interfaces which deflect and deviate nucleating and propagating cracks during static and dynamic loadings [9]. Consequently, a part of the energy required for damage of the material is consumed for propagation of cracks along the interfaces and their renucleation in every new layer.

There are several technologies for the fabrication of laminated composites. For instance, roll bonding [10–15] and diffusion (reaction) bonding [12,16,17] have been known for a long time. In several studies (e.g., [18,19]), an explosive welding technique has been proposed for fabrication of laminated composites. Formation of multilayered composites by explosive welding of either similar or dissimilar steels significantly improves their impact toughness and crack growth resistance and simultaneously increases strength [20–22]. The strengthening of explosively welded materials is due to the high-strain-rate plastic deformation of colliding plates, which is particularly strong near the interfaces [18,23].

Thus, application of explosive welding for the formation of layered titanium-based composites may be an efficient strategy for the fabrication of high-strength, lightweight, and reliable structural materials. The aim of this study is the fabrication of a high-strength Ti-based composite with enhanced impact toughness by a single-step explosive welding technique. The structure and properties of the composite are discussed.

2. Materials and Methods

The seven-layer composite was produced by explosive welding according to the parallel scheme with a stand-off distance of 1 mm (Figure 1). Four plates of VT23 and three plates of VT14 titanium alloys were used as initial materials. Both materials belong to the martensitic $\alpha + \beta$ titanium alloys but have different quantities of β stabilizers. The elemental composition of plates is shown in Table 1. The thicknesses of VT23 and VT14 were 1.5 and 0.6 mm, respectively; dimensions of the welded workpieces were 50 mm × 100 mm. A 30 mm thick layer of ammonite 6ZhV was used as an explosive.

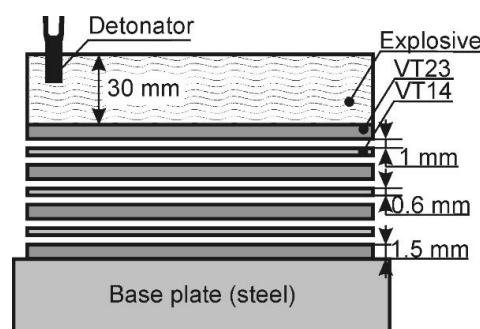


Figure 1. Scheme of the explosive welding of the seven-layer composite.

Table 1. The elemental composition of initial materials, wt %.

| Titanium Alloy | Ti | Fe | Cr | Mo | V | Al | Others |
|----------------|------|------|------|------|------|------|--------|
| VT23 | Bal. | 0.56 | 0.85 | 1.74 | 4.58 | 4.54 | 0.43 |
| VT14 | Bal. | 0.29 | - | 3.10 | 1.45 | 4.91 | 0.76 |

Structural investigations were carried out using an AxioObserver Z1m (Carl Zeiss, Oberkochen, Germany) optical microscope and an EVO 50 XVP (Carl Zeiss) scanning electron microscope (SEM) equipped with an energy-dispersive X-ray (EDX) analyzer. Samples for structural investigations were cut out along the direction of a collision point velocity and were mounted in polymer material using a SimpliMet 1000 (Buehler, Uzwil, Switzerland) hot mounting press. Preparation of the sample surfaces was carried out according to a standard procedure consisting of grinding by abrasive SiC papers with grain size varying from 100 to 5 μm and polishing by alumina with a grain size of 3 μm . Fine polishing was carried out using a colloidal silica solution with a grain size of 0.04 μm . Grinding and polishing was carried out using LaboPol-5 (Struers, Cleveland, OH, USA) equipment. The microstructure of the titanium alloys was revealed by etching with a solution of 5% HNO_3 , 3% HCl , and 2% HF in water. The fine structure of the interfaces and adjacent material was studied using a Tecnai G2 20 transmission electron microscope (TEM). For preparation of TEM specimens, Gatan Dimple Grinder Model 656 and Gatan PIPS Model 691 equipment were used.

Microhardness profiles were measured using a 402 MVD (Wolpert Group, Bretzfeld, Germany) semi-automatic microhardness tester. The load on the diamond indenter was 50 g. The mechanical properties of the material were estimated by means of tensile tests and impact tests. Tensile strength was determined using an Instron 3369 testing machine. The dimensions of the samples were 100 mm \times 8 mm \times 4 mm. The samples were loaded in the direction parallel to the interfaces. The average value of tensile strength was calculated based on the results of 5 measurements. Impact toughness was measured using a Metrocom impact testing machine with the maximum impact energy of 300 J. V-notched Charpy samples with dimensions of 55 mm \times 10 mm \times 5 mm were prepared for testing. Load was applied in the direction perpendicular to the interfaces (in the crack-arrester orientation).

3. Results and Discussion

3.1. Structural Investigations of the Interfaces Between Titanium Alloys

The explosive welding process led to the formation of a seven-layer composite consisting of alternatively stacked VT23 and VT14 layers (Figure 2). The morphology of the interfaces of the explosively welded dissimilar titanium alloys was wavy and was characterized by the presence of vortices in local areas of the welds. Variations in the wave amplitude (A) and the wave length (λ) with the interface number are shown in Figure 3a. It can be noticed that A and λ values periodically increase and decrease but, finally, these dependences are decaying. The periodical variation of A and λ can be explained in the following way. Hokamoto et al. [24] showed that in a single-shot multilayer welding, A and λ parameters depend linearly on the kinetic energy lost during collision of the plates (ΔKE). ΔKE can be found using the following equation [25]:

$$\Delta KE = \frac{m_D m_C V_p^2}{2(m_D + m_C)} \quad (1)$$

where m_D is the mass of the flyer plates per unit area, m_C is the mass of the collided plates per unit area, and V_p is the collision velocity. It is clear that for each new interface, the m_D value will be greater than for the previous one.

The collision plate velocity V_p decreases for each new interface according to the following equation [24]:

$$V_{P2} = \frac{m_D}{m_D + m_C} V_{P1} \quad (2)$$

where V_{P1} is the collision velocity at the current interface, and V_{P2} is the collision velocity at the next interface. Thus, the collision velocity is smaller for each new layer. If the mass of each plate is the same, then ΔKE will gradually decrease with the interface number. However, since at even and odd interfaces the mass of the collided plate m_C is different due to the different thicknesses of the VT23 and VT14 plates,

the ΔKE value will oscillate as shown in Figure 3b. Figure 3c shows a plot of λ versus ΔKE , which illustrates that λ has roughly linear dependence on ΔKE with some deviation for large values of ΔKE .

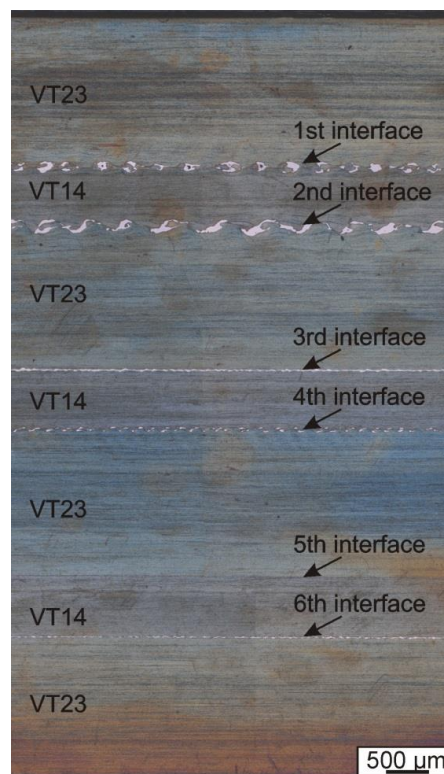


Figure 2. Panoramic view of the composite cross section.

During explosion welding, high pressure and strain rates, as well as high heating and cooling rates, are achieved at the collision point. This induces substantial structural transformations in the material adjacent to the interfaces. Particularly, formation of a severely deformed structure and vortices (or remelted zones) was observed.

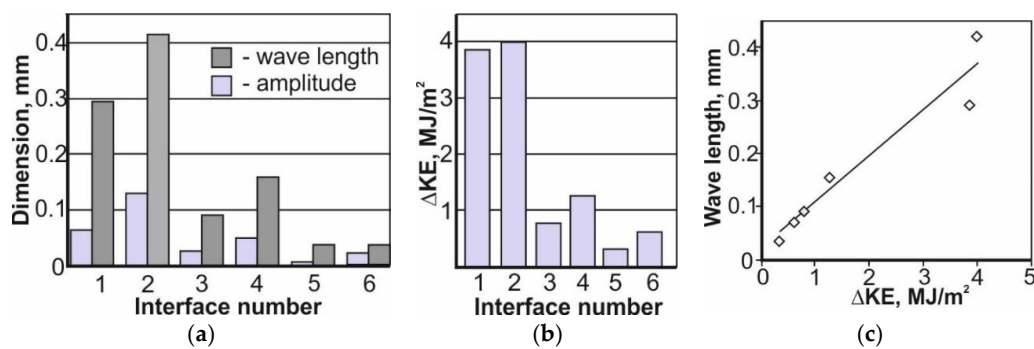


Figure 3. Amplitude, wave length (a), and kinetic energy loss (ΔKE) (b,c) for different interfaces.

High strain rate and severe plastic deformation led to the formation of highly elongated grains and shear bands (Figure 4). Localized shear bands often appear during dynamic loading of materials, for instance, during high-speed collision of metallic plates [26]. Formation of these bands typically occurs in materials with low work hardenability, low thermal conductivity, high strain rate sensitivity, and high propensity for thermal softening [27]. Titanium and its alloys comply fully with the aforementioned requirements and adiabatic shearing is a natural response of these alloys on dynamic loading. Shear bands predominantly appeared at the first, second, and third plates, which were

subjected to the highest load during explosive welding. One may notice (Figure 4a), that separation between shear bands considerably decreased near the boundary between the plates. In the vicinity of the interface, the separation between individual shear bands almost vanished, and narrow shear bands merged in thicker bands, which arranged themselves parallel to the interface (Figure 4c). TEM investigations revealed locally deformed areas adjacent to the less-strained material (Zone 1 and Zone 2 in Figure 5, respectively). Shear bands were characterized by elongation of titanium grains in the strain direction (Figure 5, Zone 1). A similar phenomenon was observed by authors of [28] when studying shear banding in Ti6Al4V. The small size of crystallites in shear bands compared to the neighboring grains gives evidence about the formation of subgrains. The mechanism of the structure formation in shear bands was suggested by several authors including Meyers et al. [29]. According to their model, the deformation starts with the homogeneous distribution of dislocations, which further rearranges itself into elongated dislocation cells. This process is known as dynamic recovery. As the deformation continues and the misorientation increases, these cells become elongated subgrains. Eventually, the elongated subgrains break up into approximately equiaxed micrograins. However, in our case, dynamic recrystallization did not take place. This means that titanium during explosive welding was subjected to subrecrystallization strains. Attributes of deformation were also observed in Zone 2 (Figure 5). This area was saturated with dislocations. In this picture, one can observe dislocation tangles as well as more energetically favorable dislocation distribution such as dislocation walls. It worth noting that shear banding did not induce any phase transformations in Zone 1 which is clearly seen in the diffraction pattern (Figure 5). The phase composition of the material in the shear bands and in the adjacent material was identical and corresponded to the mixture of α - and β -Ti (Figure 5).

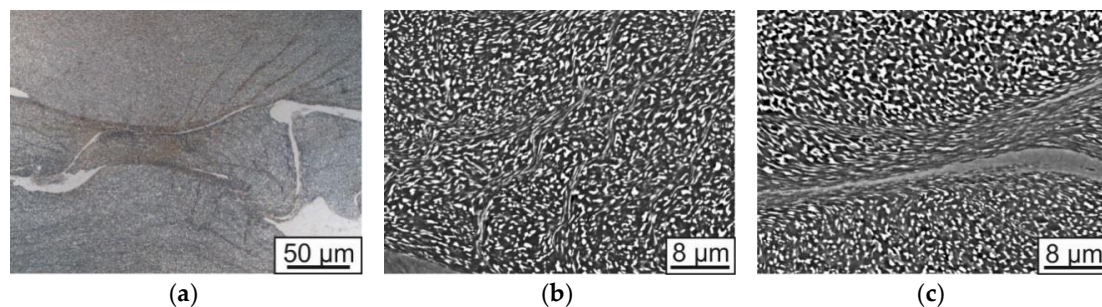


Figure 4. Shear bands near the VT23–VT14 interfaces obtained by explosive welding: (a) light microscopy image; (b,c) Scanning electron microscope (SME) images.

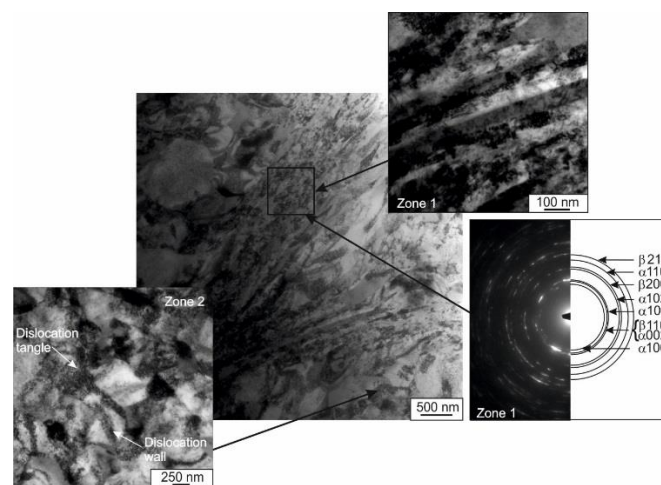


Figure 5. Results of transmission electron microscope (TEM) investigations of the shear bands and adjacent material.

The other particularity of interfaces consisted of the formation of mixing zones (Figure 6a,b). Due to turbulent movement of the material during mixing, these areas are commonly called “vortices”. The results of EDX analysis confirmed the mixing of the two alloys in vortices (Table 2). The mixing zone contained intermediate amounts of alloying elements in comparison with the VT23 and VT14 alloys. The largest number of vortices was observed at the upper wavy interfaces. Several hypothetical mechanisms of vortex formation are proposed; nevertheless, none of them is generally accepted. However, it is quite obvious that formation of vortices is associated with severe plastic deformation of the material at the collision zone, heating of local zones up to temperatures exceeding the temperature of $\alpha \rightarrow \beta$ transformation (880 ± 50 °C) and, probably, the melting temperature of titanium alloys, and subsequent rapid cooling. The combination of aforementioned processes led to martensite formation upon cooling of the vortices (Figures 6 and 7a). The formation of a needle-like structure is typically attributed to the metastable hexagonal (α') phase or martensitic orthorhombic phase (α''). Rapid cooling may lead to formation of a metastable phase along with a stable phase [30]. Electron diffraction patterns obtained from separate crystals show existence of β -Ti and α' -Ti crystals with different orientations respective to the β phase in vortex zones (see Figure 7b). Analysis of continuous cooling transformation (CCT) diagrams for titanium alloys indicates that formation of α'' phase and α' phase in VT23 and VT14, respectively, occurs when the cooling rate of vortices exceeds 10^2 K/s. Results of the numerical simulation presented in [31] indicated that the cooling rate during the explosive welding process could reach 10^7 K/s. This cooling rate is 5 orders of magnitude higher than the temperature necessary for metastable α'' -Ti and α' -Ti formation. However, only α' -Ti was observed in vortices due to the dilution of VT23 with titanium from VT14 in mixing zones. Thus, the quantity of β stabilizers in the vortex alloy was not enough for formation of α'' -Ti.

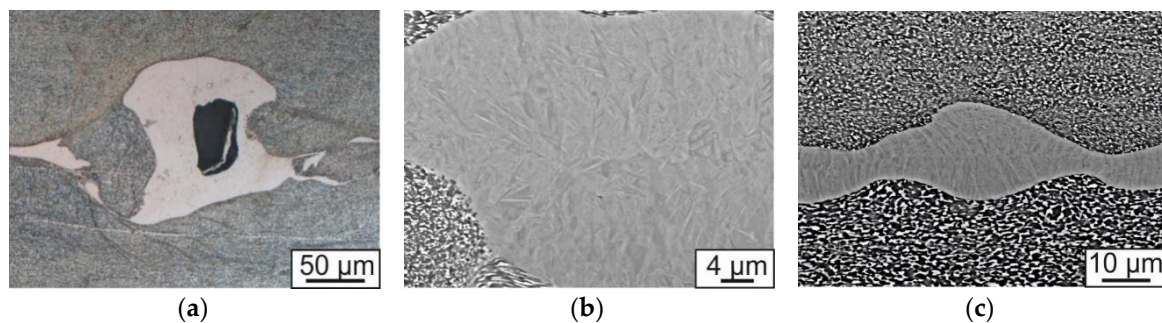


Figure 6. Quenched structure of vortices formed at VT23–VT14 interfaces: (a) light microscopy image; (b,c) SEM images.

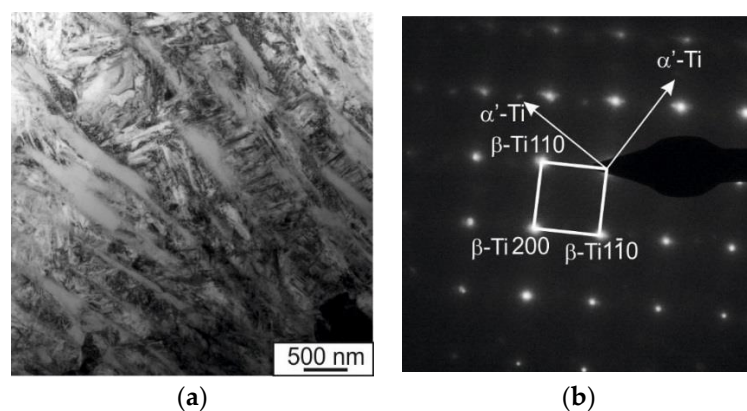


Figure 7. Results of TEM investigations of the vortex zone: (a) the structure of a vortex; (b) electron diffraction pattern obtained from the area shown in (a).

Table 2. Elemental composition of the material adjacent to the interfaces, wt %.

| Zone of Analysis | Ti | Al | V | Cr | Fe | Mo |
|------------------|-------|------|------|-----|-----|------|
| VT23 | 86.12 | 4.68 | 4.81 | 1.1 | 0.6 | 2.7 |
| VT14 | 91.04 | 4.2 | - | - | - | 4.76 |
| Mixing zone | 89.55 | 4.47 | 2.3 | 0.4 | - | 3.28 |

It can be supposed that temperatures in the vortices were much higher than the temperature of $\alpha \rightarrow \beta$ transformation. As was mentioned above, during the explosive welding process, the central parts of the vortices can be heated up to the melting point. This fact is confirmed by the formation of discontinuities in the middle part of some mixing zones, which may be associated with solidification shrinkage (Figure 6a). Mixing zones at the lower interfaces merged into a continuous layer with a thickness of 10–15 μm . This layer was located along the interfaces (Figure 6c). This phenomenon can be explained by the trapping of the jet. Cowan et al. [32] reported that trapping occurs in the absence of oscillation when two initially parallel plates collide. The cast structure of this layer results from the melting which is induced by the transfer of extremely high energies from the jet to the welded material. The formation of a continuous molten layer only at the lower interfaces can probably be explained by the small collision angle of the lower plates. As it was shown before (2), the collision plate velocity decrease for each new layer; consequently, the collision angle is also decreased due to its relation with the collision plate velocity via the equation [33,34]

$$\beta_n = 2\arcsin\left(\frac{V_n}{2V_{k(n-1)}}\right) \quad (3)$$

where β_n is the collision angle between two neighbor plates, V_n is the collision velocity at the interface between these plates, and $V_{k(n-1)}$ is the velocity of a contact point at the upper interface.

The above information can be summarized as follows. During the explosive welding, the intensive plastic deformation of α and β titanium grains occurred. The maximum plastic strain was reached near the VT23–VT14 interfaces as well as in the shear bands. The heat released during the deformation of plates led to increase of the temperature at the local areas of the interfaces up to the $\alpha \rightarrow \beta$ polymorphic transformation point and even higher (up to the melting temperature). The heat exchange with unaffected surrounding material provided a high cooling rate and martensitic transformation occurred which manifested in the formation of a needle-like structure and α' -Ti.

3.2. Mechanical Properties of the Composite

The distribution of microhardness across two layers is shown in Figure 8. The indentation was carried out in the direction from a VT23 plate toward a VT14 plate through the interface between titanium alloys.

The measurements did not reveal any noticeable increase of the microhardness caused by the work hardening near the interface. No significant increase of the hardness due to the presence of shear bands was observed as well. This fact can be explained by the small size of the heavily deformed areas (maximum 10 μm) which were smaller than the indenter imprint. However, a microhardness increase was observed in vortices with the martensitic structure. The average microhardness level of the vortices was 450 HV, while the microhardness of the VT23 and VT14 titanium alloys was about 345 HV.

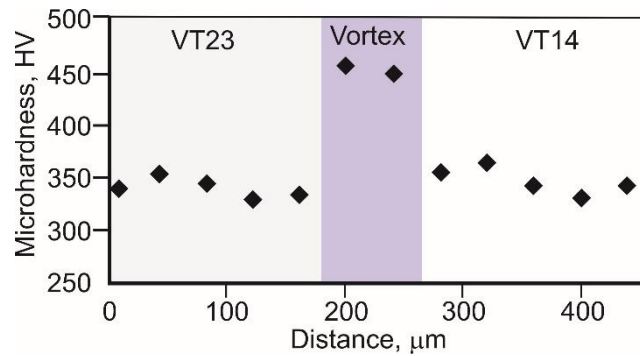


Figure 8. Results of microhardness measurements of the material near the interface between titanium alloys.

The strength of the composite was estimated based on the results of tensile tests. The impact toughness was measured during impact bending tests. The results obtained were compared with the literature data provided for initial materials (Figure 9).

The diagram (Figure 9) shows that the UTS of bulk VT23 and VT14 varies in a wide range depending on heat treatment and work hardening (from 700 to 1570 MPa for VT23 and from 835 to 1370 MPa for VT14). Average UTS values are 1075 and 1175 MPa for VT14 and VT23, respectively. The UTS of the seven-layer composite (1135 MPa) is close to these values. Thus, no significant strengthening was caused by explosive welding.

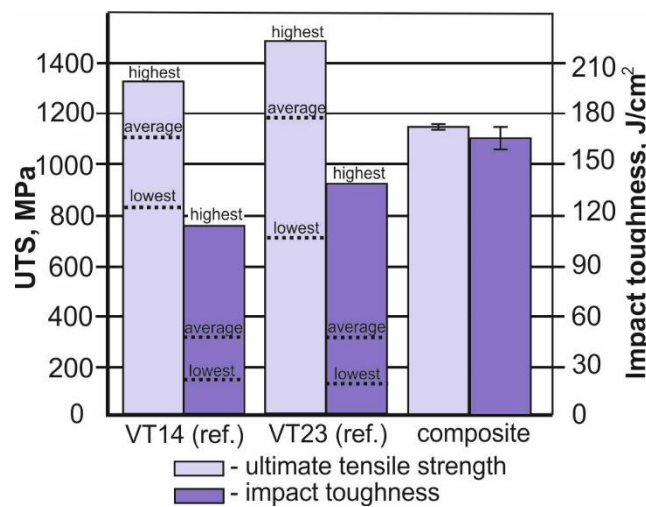


Figure 9. Results of tensile and impact bending tests of the explosively welded composite and properties of bulk VT23 and VT14 titanium alloys. The highest, the lowest, and the average values of properties of the bulk materials are calculated based on the data of Il'in et al. [7].

However, the impact toughness of the composite was 3.5-fold higher in comparison with that of the bulk titanium alloys. Similar phenomena were previously observed by Hokamoto et al. [24]. They observed a 1.7- to 4.3-fold increase of impact toughness of explosively welded carbon steel and low-carbon steel composite in comparison with its components. Kum et al. [35] and Lee et al. [36,37] observed a similar effect in ultrahigh-carbon steel laminates, and in Ni–steel and brass–steel laminates.

The impact toughness increase is typically explained by a positive influence of interfaces [35–37]. Wadsworth and Lesuer [9] describe several mechanisms of impact toughness increase in multilayered structures. Among them there are (1) crack deflection, (2) crack blunting, (3) crack bridging, (4) stress redistribution, (5) crack front convolution, and (6) local plane stress deformation. In our study we observed partial delamination of the composite, i.e., cracks propagated along the loading direction

and in the perpendicular direction. Thus, at least the first mechanism acted during the fracture. Consequently, some of the energy required for the fracture was spent for delamination and renucleation of a crack, contributing to an impact toughness increase. The main evidence for delamination is the appearance of the wavy interfaces in microphotographs (Figure 10). In the picture which demonstrates the fracture along the interface, the waves oriented perpendicular to the detonation front are clearly seen. The other regions of the fracture surface exhibited the ductile “cup and cones” mechanism of failure. Fractographic studies did not reveal any evidence of a brittle fracture along the shear bands.

Lesuer et al. mentioned that the fracture toughness increases in laminated systems with a greater amount of delamination events [38]. Delamination can be promoted by a higher number of interfaces. Consequently, one can expect an increase in impact toughness with an increase of layer quantity. In this study, we increased the impact toughness of high-strength titanium alloys by using seven layers. One can expect that an increase of number of the layers would contribute to a further increase of this characteristic. However, explosive welding of multilayer material in one step involves a number of difficulties. An increase in the layer number without an increase in the amount of explosive can lead to a weaker bonding of lower layers and decrease the quality of the multilayer materials. An increase in the amount of explosive may cause the fracturing of upper layers due to the strong plastic deformation. An approach which can be used to solve these problems is the explosive welding of a large number of metallic plates in several steps. This technology was previously successfully approved in [22] and can be successfully applied for the formation of multilayered materials with improved mechanical properties.

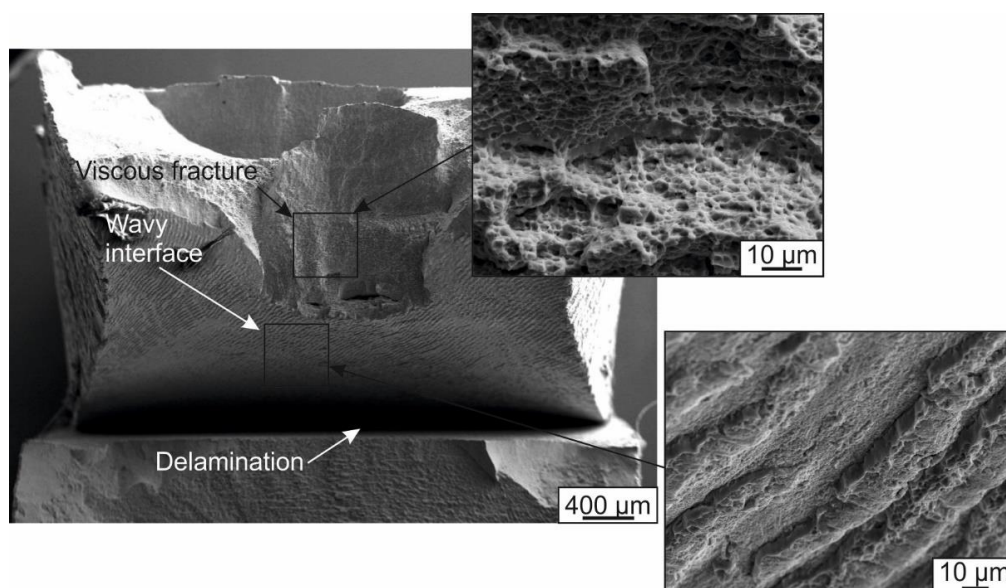


Figure 10. Fracture surfaces of VT23–VT14 multilayered materials.

4. Conclusions

Explosive welding is an efficient technology which allows the joining of several high-strength titanium plates in one step. In this study, a seven-layer laminated composite with high-quality joints was obtained. Interfaces between titanium plates possessed a typical wavy morphology. The amplitude and the wave length at the interfaces decreased in an oscillating way due to the different thicknesses of the welded plates which caused different kinetic energy losses at odd and even interfaces during explosive welding. Particularly significant structural changes occurred near the interfaces. Shear bands and the formation of vortices with a quenched structure were observed. The largest number of shear bands and vortices was observed in the upper welds which experienced higher load. The individual shear bands characterized by elongation of titanium grains merged in thicker bands near the interfaces.

The martensitic structure at the interfaces appeared due to the high temperatures of vortices and a high cooling rate (exceeding 10^2 K/s) due to heat exchange with unaffected material. Stable β -Ti and metastable α' -Ti were found in these areas. Quenched microvolumes possessed a high level of hardness (450 HV). The UTS of the composite (1135 MPa) was close to the UTS of its components. At the same time, the impact toughness of the composite was 3.5-fold higher in comparison with that of the bulk materials, which is explained by the positive influence of the interfaces.

Author Contributions: Conceptualization, D.V.L. and V.M.; Methodology, V.M.; Validation, R.K. and M.E.; Formal Analysis, I.B. and D.V.L.; Investigation, I.M., E.K., R.K. and D.V.L.; Resources, V.M. and M.E.; Data Curation, I.B.; Writing—Original Draft Preparation, D.V.L.; Writing—Review and Editing, I.B. and I.M.; Visualization, D.V.L.

Funding: This work was supported by Ministry of Education and Science of the Russian Federation according to Federal Task 11.7662.2017/BCh.

Conflicts of Interest: The authors declare no conflict of interest.

References

1. Leyens, C.; Peters, M. *Titanium and Titanium Alloys: Fundamentals and Applications*; Wiley-VCH Verlag GmbH & Co. KGaA: Weinheim, Germany, 2003; p. 532.
2. Donachie, M.J. *Titanium: A Technical Guide*, 2nd ed.; ASM International: Materials Park, OH, USA, 2000; p. 381.
3. Grabovetskaya, G.P.; Kolobov, G.P.; Ivanov, K.V.; Zabudchenko, O.V. The effect of cold severe plastic deformation on structure, deformation behavior and mechanical properties of ultrafine-grained titanium. *Phys. Mesomech.* **2004**, *7*, 22–25.
4. Grabovetskaya, G.P.; Chernova, L.V.; Kolobov, Y.R.; Girsova, N.V. Structure and deformation behavior of submicrocrystalline titanium at creep. *Phys. Mesomech.* **2002**, *5*, 87–94.
5. Dudarev, E.F.; Bakach, G.P.; Grabovetskaya, G.P.; Kolobov, Y.R.; Kashin, O.A.; Chernova, L.V. Plastic deformation behavior and localization in submicrocrystalline titanium at meso- and macroscale levels. *Phys. Mesomech.* **2001**, *4*, 97–104.
6. Dudarev, E.F.; Pochivalova, G.P.; Kolobov, Y.R.; Galkina, I.G.; Kashin, O.A.; Girsova, N.V. Influence of severe plastic deformation and subsequent annealing on true grain-boundary sliding in coarse-grained and ultrafine-grained titanium. *Phys. Mesomech.* **2004**, *7*, 30–33.
7. Il'in, A.A.; Kolachev, B.A.; Pol'kin, I.S. *Titanovye Splyavy. Sostav, Structura, Svoystva*; VILS-MATI: Moscow, Russia, 2009; p. 519.
8. Çetin, A.; Krebs, J.; Durussel, A.; Rossoll, A.; Inoue, J.; Koseki, T.; Nambu, S.; Mortensen, A. Laminated metal composites by infiltration. *Metall. Mater. Trans. A* **2011**, *42*, 3509–3520. [[CrossRef](#)]
9. Wadsworth, J.; Lesuer, D.R. Ancient and modern laminated composites—From the great pyramid of gizeh to Y2K. *Mater. Charact.* **2000**, *45*, 289–313. [[CrossRef](#)]
10. Chaudhari, G.P.; Acoff, V. Cold roll bonding of multi-layered bi-metal laminate composites. *Compos. Sci. Technol.* **2009**, *69*, 1667–1675. [[CrossRef](#)]
11. Luo, J.G.; Acoff, V.L. Using cold roll bonding and annealing to process Ti/Al multi-layered composites from elemental foils. *Mater. Sci. Eng. A* **2004**, *379*, 164–172. [[CrossRef](#)]
12. Cepeda-Jiménez, C.M.; Carreño, F.; Ruano, O.A.; Sarkeeva, A.A.; Kruglov, A.A.; Lutfullin, R. Influence of interfacial defects on the impact toughness of solid state diffusion bonded Ti-6Al-4V alloy based multilayer composites. *Mater. Sci. Eng. A* **2013**, *563*, 28–35. [[CrossRef](#)]
13. Alizadeh, M.; Samiei, M. Fabrication of nanostructured Al/Cu/Mn metallic multilayer composites by accumulative roll bonding process and investigation of their mechanical properti. *Mater. Des.* **2014**, *56*, 680–684. [[CrossRef](#)]
14. Eslami, A.H.; Mojtaba Zebarjad, S.; Moshksar, M.M. Study on mechanical and magnetic properties of Cu/Ni multilayer composite fabricated by accumulative roll bonding process. *Mater. Sci. Technol.* **2013**, *29*, 1000–1005. [[CrossRef](#)]
15. Jia, N.; Zhu, M.W.; Zheng, Y.R.; He, T.; Zhao, X. Inhomogeneous deformation of multilayered roll-bonded Brass/Cu composites. *Acta Metall. Sin. (Engl. Lett.)* **2015**, *28*, 600–607. [[CrossRef](#)]
16. Korzhov, V.P.; Kiiko, V.M.; Karpov, M.I. Structure of multilayer microcomposite Ni/Al obtained by diffusion welding. *Inorg. Mater.* **2012**, *3*, 314–318. [[CrossRef](#)]

17. Harach, D.J.; Vecchio, K.S. Microstructure evolution in metal-intermetallic laminate (MIL) composites synthesized by reactive foil sintering in air. *Metall. Mater. Trans. A* **2001**, *32*, 1493–1505. [[CrossRef](#)]
18. Ege, E.S.; Inal, O.T.; Zimmerly, C.A. Response surface study on production of explosively-welded aluminum-titanium laminates. *J. Mater. Sci.* **1998**, *33*, 5327–5338. [[CrossRef](#)]
19. Mal'tseva, L.A.; Tyushlyaeva, D.S.; Mal'tseva, T.V.; Pastukhov, M.V.; Lozhkin, N.N.; Inyakin, D.V.; Marshuk, L.A. Metallic layered composite materials produced by explosion welding: Structure, properties, and structure of the transition zone. *Russ. Metall.* **2014**, *10*, 817–825. [[CrossRef](#)]
20. Prikhodko, E.A.; Bataev, I.A.; Bataev, A.A.; Lozhkin, V.S.; Mali, V.I.; Esikov, M.A. The effect of heat treatment on microstructure and mechanical properties of multilayered composites welded by explosion. *Adv. Mater. Res.* **2012**, *535–537*, 231–234. [[CrossRef](#)]
21. Bataev, I.; Bataev, A.; Mali, V.; Burov, V.; Golovin, E.; Smirnov, A.; Prikhodko, E. Structure and fatigue crack resistance of multilayer materials produced by explosive welding. *Adv. Mater. Res.* **2011**, *287–290*, 108–111. [[CrossRef](#)]
22. Bataev, I.; Bataev, A.; Mali, V.; Esikov, M.; Bataev, V. Peculiarities of weld seams and adjacent zones structures formed in process of explosive welding of sheet steel plates. *Mater. Sci. Forum* **2011**, *673*, 95–100. [[CrossRef](#)]
23. Akbari Mousavi, S.A.A.; Al-Hassani, S.T.S.; Atkins, A.G. Bond strength of explosively welded specimens. *Mater. Des.* **2008**, *29*, 1334–1352. [[CrossRef](#)]
24. Hokamoto, K.; Chiba, A.; Fujita, M.; Izuma, T. Single-shot explosive welding technique for the fabrication of multilayered metal base composites: Effect of welding parameters leading to optimum bonding condition. *Compos. Eng.* **1995**, *5*, 1069–1079. [[CrossRef](#)]
25. Manikandan, P.; Hokamoto, K.; Deribas, A.A.; Raghukandan, K.; Tomoshige, R. Explosive welding of titanium/stainless steel by controlling energetic conditions. *Mater. Trans.* **2006**, *47*, 2049–2055. [[CrossRef](#)]
26. Stelly, M.; Dorneval, R. Adiabatic Shearing. In *Metallurgical Application of Shock-Wave and High-Strain-Rate Phenomena*; Murr, L.E., Staudhammer, K.P., Mayers, M.A., Eds.; Marcel Dekker: New York City, NY, USA, 1986; pp. 607–632.
27. Cho, K.; Chi, Y.C.; Duffy, J. Microscopic observations of adiabatic shear bands in three different steel. *Mater. Trans. A* **1990**, *21*, 1167–1675.
28. Peirs, J.; Tirry, W.; Amin-Ahmadi, B.; Coghe, F.; Verleysen, P.; Rabet, L.; Schryvers, D.; Degrieck, J. Microstructure of adiabatic shear bands in Ti6Al4V. *Mater. Charact.* **2013**, *75*, 79–92. [[CrossRef](#)]
29. Meyers, M.A.; Nesterenko, V.F.; LaSalvia, J.C.; Xue, Q. Shear localization in dynamic deformation of materials: Microstructural evolution and self-organization. *Mater. Sci. Eng. A* **2001**, *317*, 204–225. [[CrossRef](#)]
30. Bataev, I.A. Structure of explosively welded materials: Experimental study and numerical simulation. *Obrab. Metallov: Metal. Work. Mater. Sci.* **2017**, *4*, 55–67. [[CrossRef](#)]
31. Bataev, I.A.; Lazurenko, D.V.; Tanaka, S.; Hokamoto, K.; Bataev, A.A.; Guo, Y.; Jorge, A.M., Jr. High cooling rates and metastable phases at the interfaces of explosively welded materials. *Acta Mater.* **2017**, *135*, 277–289. [[CrossRef](#)]
32. Cowan, G.R.; Holtzman, A.H. Flow configurations in colliding plates: Explosive bonding. *J. Appl. Phys.* **1963**, *34*, 928–939. [[CrossRef](#)]
33. Deribas, A.A. *Fizika Uprochneniya I Svarki Vzryvom*; Nauka: Novosibirsk, Russia, 1980; p. 221.
34. *Fizika Vzryva*; Fizmatlit: Moscow, Russia, 2004; Volume 2, p. 656.
35. Kum, D.W.; Oyama, T.; Wadsworth, J.; Sherby, O.D. The impact properties of laminated composites containing ultrahigh carbon (UHC) steels. *J. Mech. Phys. Solids* **1983**, *31*, 133–137. [[CrossRef](#)]
36. Lee, S.; Oyama, T.; Wadsworth, J.; Sherby, O.D. Impact properties of a laminated composite based on ultrahigh carbon steel and brass. *Mater. Sci. Eng. A* **1992**, *154*, 133–137. [[CrossRef](#)]
37. Lee, S.; Wadsworth, J.; Sherby, O.D. Impact properties of a laminated composite based on ultrahigh carbon steel and a Ni-Si-Steel. *J. Eng. Mater. Technol.* **1992**, *114*, 278–281. [[CrossRef](#)]
38. Lesuer, D.R.; Wadsworth, J.; Riddle, R.A.; Syn, C.K.; Lewandowski, J.J.; Hunt, W.H. Toughening mechanisms in Al/Al-SiC laminated metal composites. *MRS Proc.* **2011**, *434*, 205. [[CrossRef](#)]

